Raman conversion in intense femtosecond Bessel beams in air

Maik Scheller, Xi Chen, Gombojav O. Ariunbold, Norman Born, Jerome Moloney, Miroslav Kolesik, and Pavel Polynkin*
College of Optical Sciences, The University of Arizona, 1630 East University Boulevard, Tucson, Arizona 85721, USA
(Received 24 November 2013; published 5 May 2014)

We demonstrate experimentally that bright and nearly collimated radiation can be efficiently generated in air pumped by an intense femtosecond Bessel beam. We show that this nonlinear conversion process is driven by the rotational Raman response of air molecules. Under optimum conditions, the conversion efficiency from the Bessel pump into the on-axis propagating beam exceeds 15% and is limited by the onset of intensity clamping and plasma refraction on the beam axis. Our experimental findings are in excellent agreement with numerical simulations based on the standard model for the ultrafast nonlinear response of air.

DOI: 10.1103/PhysRevA.89.053805 PACS number(s): 42.65.Dr, 42.65.Jx, 42.65.Re

I. INTRODUCTION

Studies of nonlinear optic interactions at extreme intensities in gases are motivated by potential applications in diverse fields ranging from laser particle acceleration [1] to weather control [2]. Remote atmospheric sensing is the application that would particularly benefit from efficient generation of wavelength-agile and directional optical radiation in air.

In this paper we report experiments on and numerical simulations of the efficient conversion of an intense femtosecond Bessel beam in air into bright and directional radiation propagating along the beam axis. The conversion process is shown to be driven by the delayed rotational Raman response of air molecules. For the conversion to be efficient, the incoming femtosecond Bessel beam needs to be appropriately temporally chirped. Also, the process needs to be seeded by radiation propagating along the beam axis, although the amount of the necessary seed is very insignificant. The conversion efficiency, under optimum conditions, exceeds 15% relative to the pulse energy of the input Bessel beam. The center wavelength of the on-axis generated beam can be straightforwardly tuned by terminating the interaction, at a particular point along the Bessel zone, with an aperture. Our experimental results are in excellent agreement with numerical simulations based on the standard model of ultrafast nonlinear response of air, without any fitting parameters.

II. EXPERIMENTAL SETUP AND NUMERICAL MODEL

Three modifications of our experimental setup are shown in Fig. 1. The pump radiation used is produced by a Ti:sapphire laser system that operates at 800-nm center wavelength and generates 10 pulses/s, with up to 30 mJ of energy per pulse. The pump beam can be continuously attenuated using a half-wave plate followed by a reflective polarizer. The transform-limited duration of the pump pulse is about 40 fs and the pulse can be approximately linearly chirped, either negatively or positively, to the maximum duration of about 1 ps, by a detuning pulse compressor in the laser system. The quality of chirped pump pulses is monitored by frequency-resolved optical-gating measurements.

The nearly Gaussian output beam from the laser system is apertured to a diameter of 1 cm and converted into a truncated fundamental Bessel beam by focusing with a fused-silica axicon lens. The axicon has an apex angle of 179.5° and a maximum thickness of about 1 mm. At the given diameter of the apertured input beam, the length of the linear focus zone produced by the axicon focusing is about 2.5 m. A 3-mm-diam aperture placed on the optical axis of the system 4 m away from the axicon blocks the conically diverging pump beam but passes through the radiation propagating along the beam axis. To study the process of nonlinear conversion from the intense Bessel beam into the on-axis propagating radiation in the externally seeded regime, a small 45° mirror is inserted into the beam path immediately after the axicon, as shown in Fig. 1(c). The mirror directs an about 3-mm-diam seed beam, weakly focused by a planoconvex lens with the focal length of 1 m, into the linear focus zone of the Bessel pump. The seed is produced by splitting off a fraction of the pump beam, prior to the axicon focusing, and appropriately synchronizing the seed and pump pulses in time using a delay line for the seed. The waist of the weakly focused seed beam is located at a distance of about 40 cm from the axicon.

Compared to the ordinary weakly focused or collimated Gaussian beams, using an intense Bessel beam for pumping the nonlinear optic conversion in our setup can be advantageous as in that case, high optical intensity can be sustained over significant distances. The propagation of high-power Bessel beams can be essentially governed by linear optics [3]. This is in contrast with the propagation of intense bell-shaped laser beams. In the latter case, the beam undergoes focusing-defocusing cycles, as the balance between different focusing and defocusing effects involved in the beam propagation is intrinsically dynamic and unstable.

For numerical simulations of our experiments, we employ our standard ultrafast-pulse propagator code based on the unidirectional pulse propagation equation. The material response model that we use accounts for multiphoton and impact ionization of oxygen and nitrogen molecules in air and for the instantaneous and delayed nonlinearity via Kerr and rotational Raman effects. The detailed description of our model and the code can be found elsewhere [4]. The value of the nonlinear Kerr constant is set to $n_2 = 7.8 \times 10^{-20}$ cm^2/W, according to the recent measurement [5]. The delayed rotational Raman response to the combined field of the pump

*ppolynkin@optics.arizona.edu

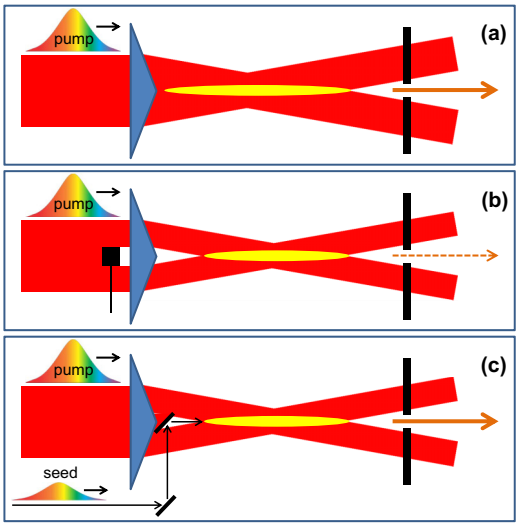

FIG. 1. (Color online) Schematics of three modifications of the experimental setup. (a) Raman generation is seeded by weak spurious on-axis beam resulting from a not perfectly pointed tip of the axicon lens. (b) The spurious seed is blocked by a small circular obstruction. (c) The on-axis beam generation is seeded externally.

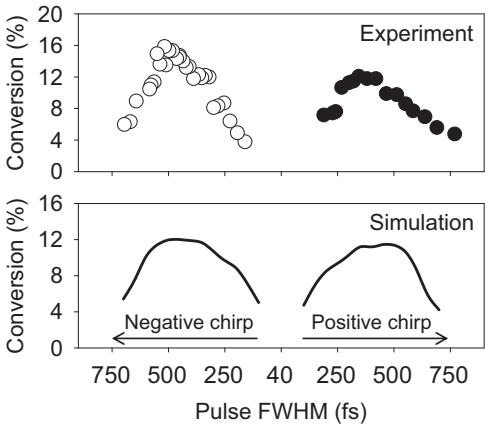

FIG. 2. The top shows the measured conversion efficiency for the spuriously seeded case, as a function of duration of the chirped 10-mJ pump pulse. The bottom shows the numerical simulation of conversion efficiency vs duration of the chirped pump pulse for the case with external seeding. The chirps of the pump and seed pulses are the same, their pulse energies are 10 and 0.2 mJ, respectively, and the delay between the pulses is set to zero immediately after the axicon.

and the copropagating amplified Raman radiation is simulated by the single damped oscillator model with frequency $\omega =$ 16 THz and decay time of 77 fs [6].

III. RESULTS AND DISCUSSION

For the case of linear propagation of the Bessel beam in our setup, about 2% of the input beam energy, after the axicon, propagates along the optical axis and is detectable past the aperture in the far field. This on-axis propagating radiation results from a nonideally sharp tip of the axicon lens, as discussed in [7,8]. In the case of nonlinear propagation with multiple-mJ level of pulse energy in the Bessel beam and no external seeding, about the same fraction of 2% of the pump energy is detected in the far field when the pump pulse is fully temporally compressed. However, when the pump pulse energy is fixed and its temporal chirp is gradually increased, the energy of the on-axis propagating beam in the far field first steadily grows with the duration of the chirped pulse, then reaches a maximum at a specific pulse duration, and finally declines. For the particular case of 10-mJ pump energy, the maximum conversion efficiency into the on-axis propagating beam is over 15%, relative to the energy of the pump beam. This maximum conversion efficiency is achieved when the duration of the chirped pump pulse is about 500 fs for both positive and negative signs of the chirp, as shown in the top part of Fig. 2.

Efficient conversion from the chirped Bessel pump into the on-axis propagating beam occurs without application of any external seed. However, strictly speaking, the conversion process is not spontaneous. If the central part of the axicon is masked by an obstruction with a diameter of about 1 mm, placed immediately after or immediately before the axicon lens, as illustrated in Fig. 1(b), the on-axis radiation in the far field vanishes. Thus the spurious on-axis seeding that, in our case, results from a nonideally sharp tip of the axicon lens is essential for efficient nonlinear conversion from the pump beam into the on-axis propagating radiation.

In the bottom part of Fig. 2 we show the results of numerical simulations for the case corresponding to the experimental data shown in the top part of the figure. In the simulation it is assumed that a collimated, 1-mm-diam, 0.2-mJ seed beam is applied. The temporal chirps of the pump and seed pulses are assumed to be the same and the delay between the two pulses immediately after the axicon lens is set to zero. The agreement between experiment and simulation is excellent. We have verified by extensive simulations that the effect of seeded generation of the on-axis propagating beam is extremely robust with respect to variations of energy of the seed pulse, its temporal chirp, and the delay between pump and seed pulses. Note, however, that the presence of the nonzero seed is essential for the generation of the on-axis beam. When the seed beam in the simulation is turned off entirely, the on-axis propagating radiation in the far field vanishes, just like it does in the experiment with the masked-off central part of the axicon. Also note that the group walk-off between the pump and signal beams in our experimental geometry is about 15 fs, which is much smaller than the duration of the pulses under the conditions for maximum seed amplification.

In Fig. 3 we show experimental and numerical data for the spectrum of the generated on-axis beam as a function of the propagation distance measured from the location of the axicon lens. The experimental data are taken by locally terminating the interaction zone with a 1-mm-diam aperture placed on the beam axis, at various longitudinal positions, and measuring the spectra of radiation transmitted by the aperture and reaching far field. Both experimental and numerical data show that the spectrum of the generated on-axis emission experiences a continuous redshift as the on-axis beam is generated and amplified along the linear focus zone of the Bessel pump beam.

The phase-matching length between the conical pump and the on-axis seed beams in our setup is about 40 cm. The

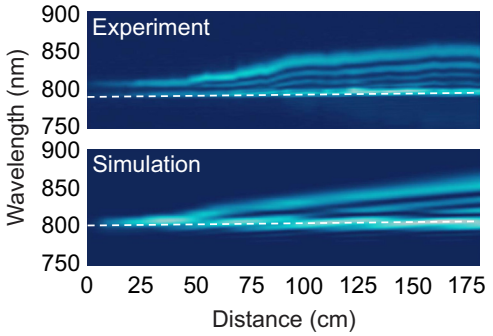

FIG. 3. (Color online) Measured and numerically simulated spectra of the on-axis emission along the interaction zone, under the same conditions as those used in Fig. 2, and for the particular value of negative temporal chirp of the pump pulse that results in the maximum conversion into the on-axis propagating beam (500 fs).

resulting periodic 2π phase slips that occur every $\sim$40 cm result in the generation of distinct spectral branches that are evident in the spectral maps shown in Fig. 3.

The observed continuous redshift of the generated on-axis signal suggests that the nonlinear conversion process is driven by the delayed Raman response of air. To confirm this conclusion, we experimentally investigated the conversion process in the externally seeded regime, as shown in Fig. 1(c). Note that in this case the center part of the axicon is masked off by the small turning mirror for the external seed, therefore the spurious seed beam that results from the blunt tip of the axicon is blocked.

An example of the measured conversion efficiency vs the delay between the seed and pump pulses is shown in the top part of Fig. 4. The results of the corresponding numerical simulation shown in the bottom part of the figure are in excellent agreement with the experiment. In the case

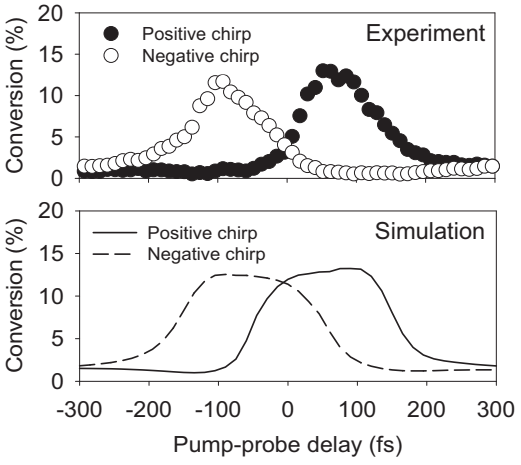

FIG. 4. Measured and numerically simulated efficiency of conversion from the Bessel pump to the on-axis generated beam, for the case with external seeding, vs seed-pump delay. The two curves on each plot correspond to two opposite signs of temporal chirp of the pump and seed pulses. In both cases, the pump and seed pulses are chirped to 500-fs duration and their energies are 10 and 0.2 mJ, respectively.

shown, the pump and seed pulse energies are 10 and 0.2 mJ, respectively, and both pulses are chirped to the duration of 500 fs. The two curves in the figure correspond to two opposite signs of the chirp.

In a temporally chirped pulse, different frequency components are separated in time. For efficient Raman conversion in the seeded case to take place, different frequency components of the pump and seed pulses that overlap in time need to differ in frequency by the Raman shift frequency, which in air corresponds to the wavelength shift of 5.4 nm [6]. From the experimental and numerical data shown in Fig. 4, the value of the seed-pump delay that results in the maximum seed amplification is about $\pm$80 fs for positively or negatively chirped pulses, respectively. The bandwidth of the chirped pulses in our setup is about 30 nm and for the case shown in Fig. 4 the pulses are chirped, either positively or negatively, to 500-fs duration. Given that rate of chirp, the observed optimum delay of 80 fs corresponds to the wavelength shift between temporally overlapping components of the pump and seed pulses of about 5 nm, which is very close to the value of the effective rotational Raman shift of air. We have verified that if the pulse chirp is varied, the temporal delay between the pump and seed pulses needs to be adjusted in order to maintain the temporal overlap between the appropriate spectral components of the pump and seed pulses, resulting in maximum energy conversion from the pump into the seed beam.

When the delayed Raman contribution to the nonlinear response of air is removed from the model, the on-axis generated wave produced by the simulation disappears, as expected. The yield of Raman conversion scales with intensity of the Bessel pump beam in the interaction zone. However, this intensity cannot be made arbitrarily high; it is limited by the sharp onset of ionization of air with the associated defocusing and scattering losses for the pump field. This is the essence of the effect referred to as intensity clamping [9]. The role of the temporal chirp of the pump pulse is to keep the on-axis intensity of the pump beam right at the highest allowed level, at the same time avoiding excessive losses to scattering on the generated plasma. If the chirp is too high, the peak intensity of the pump is low and Raman conversion is inefficient. If the chirp is too low, plasma is generated on the beam axis resulting in increased diffraction and scattering losses for the pump beam. The pump intensity is clamped at the highest

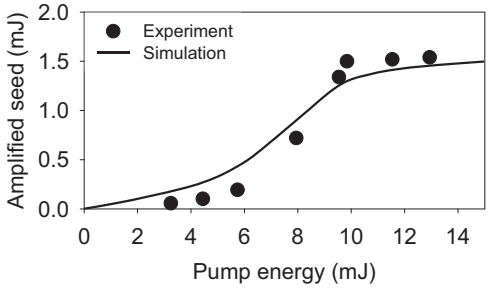

FIG. 5. Experimental and numerical data for the energy of the on-axis generated beam vs energy of the Bessel pump, for the case of externally seeded conversion. The duration of the negatively chirped pump and seed pulses is 500 fs and the delay between the pulses is optimized to maximize the amplification of the seed.

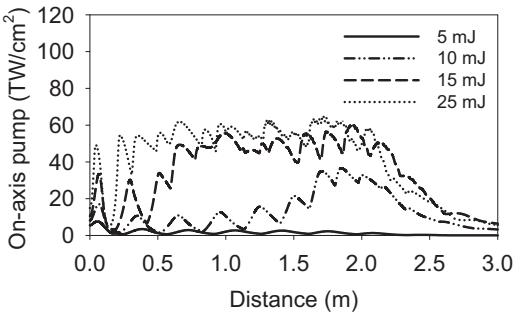

FIG. 6. Numerically simulated on-axis intensity for different energies of the pump pulse. For every case shown, the energy of the seed pulse is 2% of the energy of the pump. The pulses are negatively chirped to 500-fs duration and the delay between the pulses is adjusted to maximize the amplification of the seed.

allowed level, but some fraction of the pump energy is lost into scattering. Raman conversion is again not at its highest possible level. Thus an optimum value of the temporal chirp exists—whether it is positive or negative does not matter—that maximizes the energy of the on-axis beam generated through Raman conversion.

In Fig. 5 we show the results of experiments and numerical simulations of conversion efficiency from the Bessel pump into the on-axis seed beam for different values of pump energy. The input energy of the seed pulse is 2% of the energy of the pump pulse. Both pump and seed pulses are negatively chirped to 500-fs duration and the delay between the pulses is optimized to maximize seed amplification. As evident from the data, the energy of the on-axis beam saturates when the pump-pulse energy exceeds about 10 mJ. The reason for the saturation becomes evident from the analysis of the numerical data for the peak on-axis intensity of the Bessel pump beam, along the interaction zone, for different values of pump energy, shown in Fig. 6. According to those data, the peak intensity becomes clamped when the pump energy exceeds about 15 mJ, close to the value at which the energy of the on-axis generated beam saturates. The intensity clamping is caused by the onset of plasma generation on the beam axis and the level of the clamped intensity in this case is about 50 TW/cm^2, which is similar to that reported for ordinary femtosecond laser filaments in air [9]. Noticeable oscillations of the on-axis intensity along the Bessel zone are caused by the interference between the conical Bessel beam and the on-axis propagating amplified seed, as discussed in [8].

IV. SUMMARY AND CONCLUSIONS

In conclusion, we have demonstrated an efficient remote generation of bright and nearly collimated radiation through Raman conversion pumped by an intense femtosecond Bessel beam in air. The generation of the on-axis beam is, strictly speaking, not spontaneous and relies on the application of a weak external seed beam. However, the effect is extremely robust with respect to the variations of the energy and temporal chirp of the seed pulse, as well as to its delay relative to the pump pulse. The conversion efficiency from the Bessel pump into the on-axis propagating radiation exceeds 15%. It is shown to be limited by the onset of plasma-driven intensity clamping for the pump beam in the interaction zone. The wavelength of the on-axis generated beam can be straightforwardly controlled through terminating the interaction, at a particular location along the Bessel zone, with an aperture. Numerical simulations based on the standard ultrafast response of air are in excellent agreement with our experimental results. The reported effect may be useful in remote atmospheric sensing.

ACKNOWLEDGMENTS

The authors acknowledge helpful discussions with Ewan Wright. This work was supported by The United States Air Force Office of Scientific Research under Grants No. FA9550-12-1-0143, No. FA9550-12-1-0482, and No. FA9550-10-1-0561 and by The United States Defense Threat Reduction Agency under Grant No. HDTRA1-14-1-0009.

[1] A. G. York, H. M. Milchberg, J. P. Palastro, and T. M. Antonsen, Phys. Rev. Lett. **100**, 195001 (2008).
[2] J. Kasparian *et al.*, Opt. Express **16**, 5757 (2008).
[3] P. Polynkin, M. Kolesik, A. Roberts, D. Faccio, P. Di Trapani, and J. V. Moloney, Opt. Express **16**, 15733 (2008).
[4] M. Kolesik and J. V. Moloney, Phys. Rev. E **70**, 036604 (2004).
[5] J. K. Wahlstrand, Y.-H. Cheng, and H. M. Milchberg, Phys. Rev. A **85**, 043820 (2012).
[6] M. Mlejnek, E. Wright, and J. V. Moloney, Opt. Lett. **23**, 382 (1998).
[7] S. Kurilkina, A. Ryzhevich, S. bushuk, and S. Solonevich, Quantum Electron. **38**, 349 (2008).
[8] S. Akturk, B. Zhou, B. Pasquiou, M. Franco, and A. Mysyrowicz, Opt. Commun. **281**, 4240 (2008).
[9] S. Xu, J. Bernhardt, M. Sharifi, W. Liu, and S. L. Chin, Laser Phys. **22**, 195 (2012).